ELSEVIER

Journal of Photochemistry and Photobiology A: Chemistry 138 (2001) 177–183

Journal of Photochemistry and Photobiology A:Chemistry

www.elsevier.nl/locate/jphotochem

New route for degradation of chlorinated ethylenes in exhaust gases from ground water remediation

Lutz Prager*, Eberhard Hartmann

Institute for Surface Modification, Permoserstrasse 15, D-04318 Leipzig, Germany

Received 11 September 2000; accepted 23 October 2000

Abstract

On the basis of an approximate finite-size description, a UV photoreactor was devised and constructed for studying the photooxidation of the chlorinated ethylenes perchloroethylene (PCE), trichloroethylene (TCE), 1,2-dichloroethylenes (DCE), vinyl chloride (VC) and several saturated chlorinated hydrocarbons (CHC). In the cases of PCE and TCE, the efficiency of the photooxidation using irradiation by a 222 nm excimer lamp and subsequent photolysis for the initiation of the process was found to be sufficiently high so that a scaling up to an industrial purification plant of exhaust gases from ground water remediation can be hopefully envisaged. Thanks to consecutive reactions with the chain-sustaining chlorine atoms, this degradation route proves capable of decomposing the other chlorinated ethylenes which are not amenable to photolysis in a direct way. For saturated CHC the utilisability of this approach is limited. © 2001 Elsevier Science B.V. All rights reserved.

Keywords: Ground water remediation; Exhaust air; Chlorinated ethylenes; Photooxidation; Photoreactor; Excimer lamp; Finite-elements simulation

1. Introduction

Handling of chlorinated solvents in industry and trade as well as remediation of contaminated soil and ground water may produce exhaust gases charged by chlorinated hydrocarbons (CHC). In case of exceeded emission limits, these air streams must be urgently purified before releasing them into the ambient air. Perchloroethylene (PCE) and trichloroethylene (TCE) which are commonly utilised in dry-cleaning or metal degreasing plants and a few other compounds like *cis*-1,2-dichloroethylene (*cis*-DCE), vinyl chloride (VC) and 1,1,1-trichloroethane (1,1,1-TCA) which are natural degradation products of TCE and PCE in ground water and soil, form important pollutants in exhaust air in a typical concentration range from 5 to 250 ppm. So far, numerous technologies such as adsorption on activated charcoal and catalytic incineration have been elaborated and are in common use. Nevertheless, in most cases, they reveal specific shortcomings, still motivating further research.

A purification technology for exhaust air from ground water remediation is extensively discussed in [1], allowing for a mineralisation of organically bound chlorine into unperilous chlorides. It took part of its pattern from [2] and consists of three consecutive steps: (i) photooxidation of the CHC's in a photoreactor; (ii) scrubbing and hydrolysis of the water-soluble products in a conventional packed absorption column by means of caustic soda solution and, finally, (iii) thermal dechlorination of the hydrolysis products in a flow reactor. In future work, the results of this study will be used for devising a mobile pilot degradation plant.

The present paper focuses on the technological step (i) of the photooxidation. A brief survey of the photoinitiation and subsequent chain reactions is followed by the description of a simulation program for modelling the processes occurring in the photoreactor. Then, an experimental set-up is presented for studying the photodegradation with the aid of a 222 nm excimer lamp. Finally, the degradation data are given which were obtained for pure and mixed contaminants at air streams up to $450\,m^3\,h^{-1}$.

2. Methodology

2.1. Photooxidation of chlorinated ethylenes

As is generally known an oxidative degradation of unsaturated CHC's such as PCE and TCE in ambient air occurs with a high efficiency in a chain reaction which is sustained by chlorine atoms [3]. In order to exemplify this circum-

* Corresponding author. Tel.: +49-341-2352428; fax: +49-341-2352584.
E-mail address: prager@rz.uni-leipzig.de (L. Prager).

1010-6030/01/$ – see front matter © 2001 Elsevier Science B.V. All rights reserved.
PII: S1010-6030(00)00399-3

stance, start reaction and chain propagation are briefly described for the particular case of PCE where the initiation (Eq. (1)) can be achieved by photolysis using a UV lamp in the short-wavelength region below 250 nm, with the quantum yield Q being close to unity

$$CCl_2{=}CCl_2 + h\nu\,(\lambda < 250\,\text{nm}) \rightarrow {}^{\bullet}CCl{=}CCl_2 + Cl^{\bullet} \quad (1)$$

In the presence of oxygen, the chain propagation (Eqs. (2)–(6))

$$CCl_2{=}CCl_2 + Cl^{\bullet} \rightarrow {}^{\bullet}CCl_2{-}CCl_3 \quad (2)$$

$${}^{\bullet}CCl_2{-}CCl_3 + O_2 \rightarrow CCl_3{-}CCl_2OO^{\bullet} \quad (3)$$

$$CCl_3 - CCl_2OO^{\bullet} + ROO^{\bullet} \rightarrow CCl_3{-}CCl_2O^{\bullet} + RO^{\bullet} + O_2 \quad (4)$$

$$CCl_3{-}CCl_2O^{\bullet}\,(+M) \rightarrow CCl_3{-}COCl + Cl^{\bullet}\,(85\%) \quad (5a)$$

$$CCl_3{-}CCl_2O^{\bullet}\,(+M) \rightarrow COCl_2 + {}^{\bullet}CCl_3\,(15\%) \quad (5b)$$

$${}^{\bullet}CCl_3 + O_2 \rightarrow CCl_3OO^{\bullet} \rightarrow \cdots \rightarrow COCl_2 + Cl^{\bullet} \quad (6)$$

leads to the formation of about 85 trichloroacetyl chloride (TCAC) and 30 carbonyl chloride (CC) molecules from 100 PCE molecules. The trichlorovinyl radical as generated in the initiation step in Eq. (1) reacts in its turn with oxygen, yielding a second Cl atom.

$${}^{\bullet}CCl{=}CCl_2 + O_2 \rightarrow \cdots \rightarrow COCl_2 + CO + Cl^{\bullet} \quad (7)$$

The formation of two Cl atoms per initiation step accounts for the high degradation efficiency in the chain reactions (Eqs. (2)–(6)). Of course, one has also to consider chain termination which is produced by wall interaction and reactions of the radicals among themselves.

The analogous reaction scheme of TCE yields about 91 dichloroacetyl chloride (DCAC), nine CC and nine formyl chloride (FC) molecules according to reactions in Eqs. (5a), (5b) and (6), respectively. Conforming with Eq. (7) FC, CO and Cl are produced.

In principle, the outlined reaction scheme also applies to *cis*- and *trans*-DCE. The efficiency of the chain reaction is limited by the fact that oxidation of the chlorovinyl radical (emerging in the start reaction analogous to Eq. (1)) does not yield a second Cl atom.

$${}^{\bullet}CH{=}CHCl + 2O_2 \rightarrow \cdots \rightarrow HCOCl + CO + HO_2{}^{\bullet} \quad (8)$$

In the case of VC, the subsequent reactions do not produce any Cl atom. A reaction according to Eq. (5a) does not occur and Eqs. (5b) and (6) have now to be replaced by

$$CH_2Cl{-}CHClO^{\bullet}\,(+M) \rightarrow HCOCl + {}^{\bullet}CH_2Cl \quad (9)$$

and

$${}^{\bullet}CH_2Cl + \tfrac{3}{2}O_2 \rightarrow \cdots \rightarrow HCOCl + HO_2{}^{\bullet} \quad (10)$$

In most cases, the respective rate constants can be taken from the standard source [4].

Table 1
Absorption coefficients ε_{222} ($dm^3\,mol^{-1}\,cm^{-1}$) of some CHC's at 222 nm, their rate constants k_{Cl} ($10^{10}\,dm^3\,mol^{-1}\,s^{-1}$) for the reactions with Cl atoms and numbers of Cl atoms n_{Cl} formed per degradated initial molecule

CHC	ε_{222} [5]	k_{Cl} [4]	n_{Cl}
PCE	5500	3.56	2
TCE	4000	4.24	2
trans-DCE	1200	5.61	1
cis-DCE	500	5.53	1
VC	< 10	8.79	0
DCM[a]	0.15	0.02	1
1,1,1-TCA	17.8	0.0004	1

[a] DCM denotes dichloromethane.

The efficiency of the starting reaction (Eq. (1)) is determined by the absorption coefficient and the quantum yield. The absorption coefficient is wavelength-dependent and the value pertaining to 222 nm has to be chosen here because in the present investigations a KrCl* excimer lamp was used. The set of corresponding values in Table 1 reveals rather large values for PCE and TCE, bringing on a quite efficient photodissociation of these particular contaminants. In contrast to that the respective value for *cis*-DCE is smaller by 1 order of magnitude and nearly vanishes for VC. The rate constants for the Cl addition (Eq. (2)) are found to lie around $5 \times 10^{10}\,dm^3\,mol^{-1}\,s^{-1}$, leading to a diffusion-controlled reaction of chlorinated ethylenes with Cl atoms. Finally, reactions of the chlorovinyl and chloromethyl intermediates with ambient oxygen at the naturally high concentration of the latter and with rate constants around $10^9\,dm^3\,mol^{-1}\,s^{-1}$ are very fast.

Saturated CHC's such as dichloromethane (DCM) and 1,1,1-TCA absorb 222 nm photons to a much lesser extent and also their rate constants for reactions with Cl are by far to small for their efficient degradation in mixtures with Cl donors. However, such an Cl attack leads to the rate determined H abstraction under HCl formation. The chloroalkyl radical as a further product of the H abstraction reacts with ambient oxygen analogous to Eq. (6).

2.2. Photoreactor modelling

In literature, numerous computer codes exist for sophisticated evaluations of the "local volumetric rate of energy absorption" (for a survey see [6]). However, in our particular case of a contaminant highly diluted in an optically inactive carrier gas, we aim at a dense and flexible description by introducing some obvious approximations. (i) In the cylindrical photoreactor, all the radial profiles of the relevant distributions (UV lamp luminance, concentrations of all the gas constituents including the intermediates, UV photon density, gas flow rate) are smeared over the flow area which is the transversal cross section of the photoreactor. This symmetry approximation enables one-dimensional (axial) discretisation of the kinetic equations for the initiation by UV absorption and the consecutive complex chain

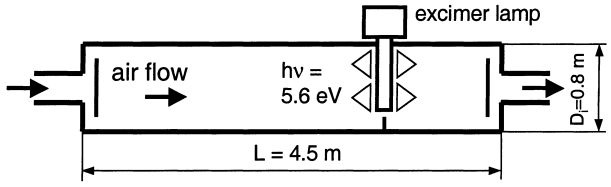

Fig. 1. The photoreactor, schematic.

reactions. (ii) The latter are optionally treated in a dense manner as an overall reaction which comprises the various actual reactions (Eqs. (1)–(7)) in an effective way within the largely phenomenological quantum yield conception. The yield values are given as constants or, optionally, in their concentration dependence. (iii) As usual, we break down the complex interplay of the simultaneous processes of UV initiation, overall disintegration of the optically active pollutant components and gas flow into consecutive fractional steps [7]. Numerical stability is achieved by calculating a suitable time increment corresponding to the actual state of the reactor. (iv) In order to attain stationary state, the calculation starts from an arbitrary reactor state, i.e. empty reactor and the UV lamp switched on. Then, gas flow and fractional reaction steps are treated iteratively until a self-consistency criterion is fulfilled. Of course, the stationary state was found to be independent on the particular starting conditions.

Providing the FORTRAN code *PHOTOR* with the reactor configuration (diameter and length, lamp position and UV power), the gas composition and flow rate as well as with kinetic data (photo cross-sections, quantum yields), the resulting stationary state is obtained within a few minutes in a common PC environment. The stationary state is represented by all the axial distributions of the concentrations of the various gas components as well as photon density.

2.3. Experimental

On the basis of the reactor simulation, a cylindrical steel reactor (inner diameter $D_i = 0.8$ m, length $L = 4.5$ m, inner surface enamelled) was constructed, with the UV excimer lamp positioned in the rear (at 3.3 m in downstream direction, cf. Fig. 1). The inlet pipe contains a heated and nitrogen purged evaporator which is provided with the pollutants under investigation by a syringe pump (Bioblock, Razel Scientific Instruments [1]), thus continuously adding the pollutants to the indoor air stream. Several baffles at inlet and outlet positions achieve efficient gas mixing and turbulence.

The UV source was a KrCl* excimer lamp (BLC 222/600-360°, Heraeus Noblelight GmbH, see footnote 1): with the aid of an ac high voltage dielectric barrier discharge an excimer gas mixture consisting of krypton and chlorine is excited inside a water-cooled cylindrical quartz tube ($l = 0.67$ m, outer diameter $D_a = 40$ mm), and UV photons are emitted with a radiant power $P_{UV} = 150$ W at a narrow wavelength band $\lambda = (222 \pm 5)$ nm [8]. The radiant power was measured in dependence on the primary current of the lamp power supply, using a radiometer (URADES 4, GERUS mbH, see footnote 1) which is equipped with a SiC photodetector. In doing so, the UV photon density was measured at a distance of 4 m and a corresponding integration yielded the total UV radiant power P_{UV}.

After UV treatment, the effluent flows through a flexible PVC tube ($D_i = 0.2$ m) into a packed absorption column which contains 1.5 M caustic soda solution as the absorbent. Then, after passing a charcoal absorber the air flows through a tube section ($L = 2$ m, $D_i = 0.2$ m) in which the flow rate is measured (452 FT-08, Kurz Instruments Inc., see footnote 1). The flow rate is controlled by a blower and a butterfly valve and can be varied in the range from 50 to 450 $m^3\,h^{-1}$. The blower brings on a slight reduction of the working pressure (by about 30 mbar below ambient pressure), thus precluding emission of hazardous contaminants and intermediates into the surroundings.

Air sampling is not only done at the entrance and the exit of the reactor by means of PTFE tubes ($D_i = 6$ mm) but, in addition to that, an axially relocatable skid enables air sampling at any position upstream from the UV lamp. At flow conditions, the gas composition was controlled by the application of FTIR spectrometry (in the wave number range from 600 to 4000 cm^{-1} with a spectral resolution of 1 cm^{-1}). The spectrometer employed (Vector 22, Bruker Analytik GmbH, see footnote 1) was equipped with a quartz cell (optical length $l = 0.2$ m) and NaCl windows. For the sake of reproducibility, long equilibration times were chosen (5–30 min). Under the particular measuring conditions the detection limits for the contaminants, intermediates and products were found to lie in the range from 0.5 to 5 ppm.

3. Results and discussion

Of course, photodegradation studies of a series of pure contaminant systems appear informative for delineating the effects of the photoinitiation efficiency (ε_{222} in Table 1), reactivity with Cl atoms (k_{Cl}) and number of Cl atoms (n_{Cl}) as formed in the course of the chain reactions. Thus, TCE and PCE efficiently absorb the 222 nm photons employed and both of them show a strong reactivity to the chain-sustaining Cl atoms. Moreover, in their degradation routes, two Cl atoms are formed in excess. The unsaturated *trans*-DCE (standing proxy for *cis*-DCE) and VC still show the high reactivity with Cl thanks to efficient Cl addition but, as compared with the ethylenes TCE and PCE, they reveal weak and negligible photo cross-sections and less effective Cl atom formations (1 and 0), respectively. The saturated CHC's DCM and 1,1,1-TCA do not reveal appreciable photoabsorption. Their interaction with the sustaining Cl atoms is due to H abstraction processes. The pertinent kinetic con-

[1] The use of commercial names to identify the materials and equipment in no way implies endorsement or recommendation by IOM.

stants k_{Cl} are rather small and multiplication of Cl atoms does not occur.

In a second step, investigation of contaminant mixtures can disclose interrelations between the various components. Thus, the strong Cl donors TCE and PCE could initiate and sustain degradation of components with small photo cross-section, at the same time retarding by the Cl donation their own chain reactions.

3.1. One-component contaminant samples

The following reagents were used as pollutants: PCE — 99% ACS reagent; TCE — 99% spectrophotometric grade; DCM — 99.9% ACS reagent; 1,1,1-TCA — 99% (all purchased from Aldrich, see footnote 1); *trans*-DCE purum (Fluka AG, see footnote 1); VC 99.5% inhibited with phenol (Chemische Werke Schkopau, see footnote 1).

Fig. 2 shows axial concentration profiles for the contaminants PCE, TCE, *trans*- and *cis*-DCE which were calculated for inflow concentrations c_0, UV radiant power P_{UV} and air flow rate V', together with some experimental data for PCE. In agreement with the experiment, the simulation yields quantitative conversion only for the strong Cl donors PCE and TCE whereas, owing to smaller photo cross-section and, more decisively, absent Cl atom multiplication, the DCE conversion is not quantitative and remaining DCE concentrations can reach the reactor exit. Due to vanishing photo cross-sections, VC, DCM and 1,1,1-TCA do not undergo any photodegradation.

The discrepancy between simulated and measured photon densities is worth mentioning which occurs particularly near the lamp, obviously being a consequence of the approximate smearing of the UV luminance over the transversal

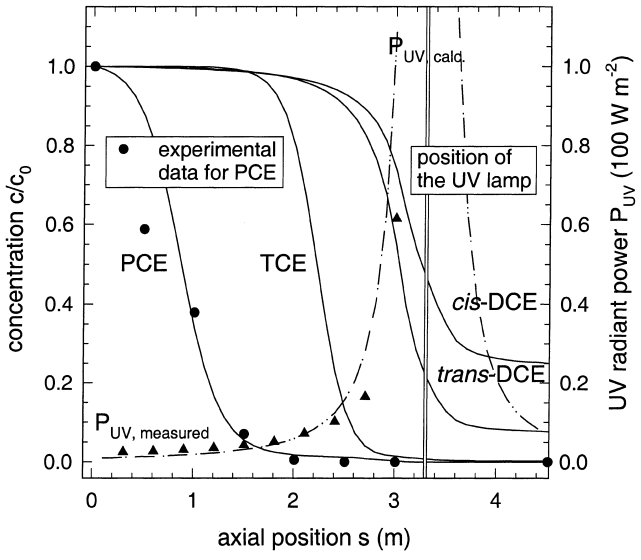

Fig. 2. Decomposition of chlorinated ethylenes. Axial profiles of pollutant concentration and UV radiant power; $c_0 = 175\,\text{ppm}$; $V' = 135\,\text{m}^3\,\text{h}^{-1}$; $P_{UV} = 150\,\text{W}$.

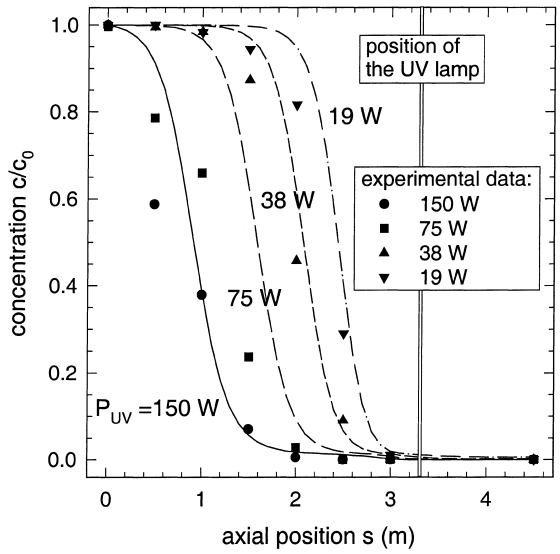

Fig. 3. Calculated and measured axial PCE concentration profiles for varying UV power; $c_{0,PCE} = 175\,\text{ppm}$, $V' = 135\,\text{m}^3\,\text{h}^{-1}$.

cross section. Note the pronounced peaking of the specific UV power in the very surroundings of the lamp. Furthermore, Fig. 2 discloses that degradation takes place within quite narrow reaction zones. More or less favourable kinetic data just cause an axial shift of the reaction zone, leaving the effluent concentrations over a wide range largely unaltered. One may conjecture that the latter finding can be generalised to the other degradation parameters, i.e. UV power P_{UV}, contaminant inflow concentration c_0 as well as flow rate V'. Indeed, as illustrated in Fig. 3, the variation of UV radiant power clearly verifies this presumption, testifying a relatively uncritical degradation behaviour with regard to variations of the aforementioned operating parameters and, hence, long-time stability of the photoreactor under industrial conditions.

In the degradation studies, we dispensed with the actinometrical measurements of the absorbed UV energy and, instead, discussed the product concentrations in dependence on the total UV radiant power.

For the ethylenes PCE and TCE, Figs. 4 and 5 show the product concentrations at the reactor exit in their dependence on UV power. In both cases, quantitative conversion is already attained at rather low UV power. PCE degradation yields TCAC, CC, CO and small amounts of HCl (not quantified). At the small UV power of 19 W, PCE is completely degraded and, in accordance with [3], TCAC and CC molecules are formed in a ratio of 85:30. In the course of further photodegradation, TCAC ($\varepsilon_{222} = 182\,\text{dm}^3\,\text{mol}^{-1}\,\text{s}^{-1}$) yields CC, CO and Cl atoms, until at high UV power ($P_{UV} = 150\,\text{W}$) TCAC and CC are obtained in a molecule ratio of 81.2:33.8. The slight TCAC decomposition is in a good agreement with *PHOTOR* simulations which predicted a TCAC degradation by about 4%.

In the TCE degradation route (Fig. 5), DCAC, CC and FC are the main products, particularly occurring at a small

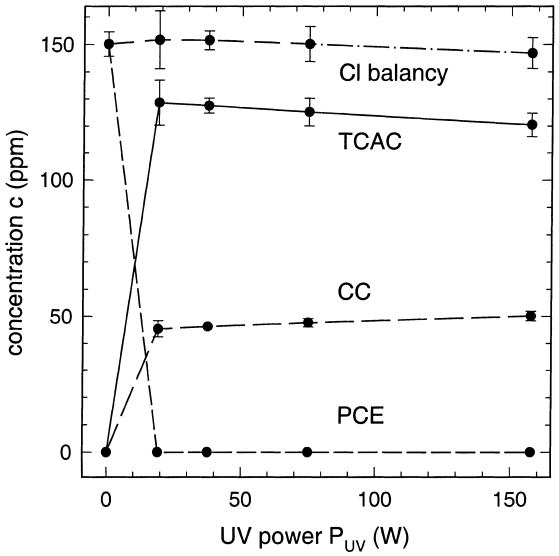

Fig. 4. Decomposition of PCE. Product concentrations in reactor effluent; $V' = 135\,m^3\,h^{-1}$; $c_0 = 150\,ppm$.

UV power ($P_{UV} = 19\,W$) at the reactor exit in the ratio 85.2:11.2:12.2 per 100 molecules converted. 6.2 CO and 5.8 HCl molecules were additionally found, readily covering the carbon and chlorine balancies. At a somewhat higher UV power ($P_{UV} = 38\,W$), TCE is virtually converted. At a high flow rate ($V' = 425\,m^3\,h^{-1}$) and small UV power ($P_{UV} = 19\,W$), the above-mentioned products (together with trifling proportions of CO and HCl) were detected near the reaction zone in a ratio of 88.6:11.1:10.5 which is nearly that one (91:9:9) as quoted in [9]. The photolytic decomposition of DCAC ($\varepsilon_{222} = 115\,dm^3\,mol^{-1}\,s^{-1}$; $Q = 1.5$ [10]) becomes manifest in the decrease of the DCAC proportion at increasing UV radiant power. CC, CO, HCl and Cl are products

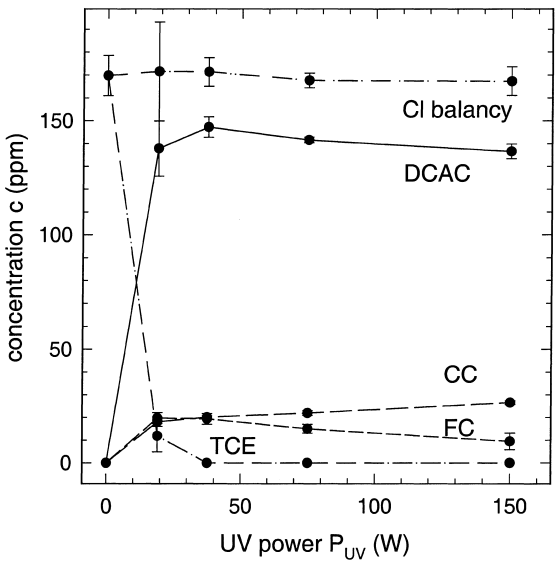

Fig. 5. Decomposition of TCE. Product concentrations in the reactor effluent; $V' = 135\,m^3\,h^{-1}$; $c_0 = 170\,ppm$.

of the DCAC degradation, with the latter potentially carrying the possibly constituting chain reaction in the DCAC decomposition ($k_{Cl+DCAC} = 2.2 \times 10^7\,dm^3\,mol^{-1}\,s^{-1}$ [9]).

Photooxidation of *trans*-DCE yields the products FC, CO, HCl, DCAC and CO_2. Under the operation conditions ($P_{UV} = 110\,W$, $V' = 135\,m^3\,h^{-1}$, $c_0 = 240\,ppm$), a significant decomposition was observed to 180 ppm (78%) and 90 ppm (37.5%) at a position near the reaction zone ($s = 2.7\,m$) and at the exit ($s = 4.5\,m$), respectively. These contents of non-converted DCE comprise *cis*-DCE proportions (e.g. 7.4 ppm at $s = 2.7\,m$) which originate from the *trans–cis* isomerisation as a result of the photoexcitation. Having in mind the approximations and potential measuring errors (e.g. HCl losses at the wall) the realistic description is surprising which *PHOTOR* can give to this particular photodegradation (cf. Fig. 2). For instance, near the reaction zone ($s = 2.7\,m$) the elemental balancies were largely covered (C 100%, Cl 97.5%) and 133 FC, 52 CO, 25 HCl, 10 DCAC and 4 CO_2 molecules were found to emerge from 100 *trans*-DCE. Photolytic degradation of FC as the prevailing product of the DCE degradation is of minor importance here ($\varepsilon_{222} = 66\,dm^3\,mol^{-1}\,s^{-1}$). Estimations with the aid of *PHOTOR* yielded decomposition rates <2%. However, FC is unstable and decomposes as a result of wall collisions and surface reactions, yielding CO and HCl.

Although some particular findings, such as the occurrence of DCAC and CC in the degradation route of *trans*-DCE are not understood, the degradation behaviour of one-component pollutants can be largely systematised on the basis of the above outlined mechanistic ideas, mainly in terms of UV absorbances, quantum yields, reactivity with Cl atoms and the recoveries of the latter atoms.

3.2. Two-component contaminant samples

With regard to photoabsorbance ε_{222}, reactivity with Cl atoms k_{Cl} and Cl recovery n_{Cl}, the unsaturated pollutants *cis*- and *trans*-DCE and VC as well as the saturated ones DCM and 1,1,1-TCA open a series of varying interaction strength with the strong Cl donors PCE and TCE (cf. Table 1).

Apart from intermediate and nearly vanishing UV absorbance ε_{222}, the DCE's and VC show rather large rate constants k_{Cl} for the Cl addition. Only the DCE's can restitute the Cl atoms to the respective donor, thus not impeding the chain degradation of the latter. Then, it is quite obvious that under the operational conditions applied ($P_{UV} = 150\,W$, $V' = 135\,m^3\,h^{-1}$) in both of the investigated *trans*-DCE/PCE mixtures ($c_{0,DCE}/c_{0,PCE}$: 38 ppm/118 ppm and 68 ppm/97 ppm) the strong Cl donor PCE fully imparts its degradation efficiency to the Cl restoring DCE component in the initiation stage, thereby leaving the consecutive chain reaction unaltered. It appears quite obvious that also in mixtures with the Cl donating TCE, an analogous degradation behaviour was observed.

As mentioned before in the photooxidation reaction of the VC pollutant no Cl atom is formed which could be

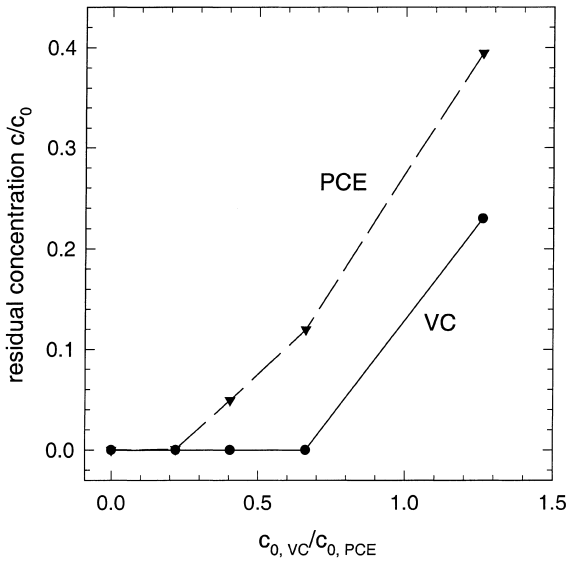

Fig. 6. Degradation of VC–PCE mixtures. Residual concentration of the components in the reactor effluent vs. concentration ratio; $P_{UV} = 150\,W$, $V' = 135\,m^3\,h^{-1}$.

restored to the Cl donating PCE, thus curtailing the chain degradation reactions of the latter. In operational conditions as applied before ($P_{UV} = 150\,W$, $V' = 135\,m^3\,h^{-1}$) for low enough concentration ratios (e.g. $c_{0,VC}/c_{0,PCE} = 34\,ppm/154\,ppm = 0.22$) such an adverse effect, however, did not occur and a quantitative conversion of both the pollutants into the products TCAC, CC, FC, CO, HCl, and CO_2 was observed. Above a threshold of about $c_{0,VC}/c_{0,PCE} = 0.25$, the Cl donor PCE can no longer sustain the degrading reactions of the Cl donee VC in addition to its own chain reaction. Consequently, with growing VC concentration the average length of the PCE chain reactions becomes increasingly shortened, bringing on unconverted pollutant concentrations to a more pronounced extent even for PCE than for the more effective Cl donee VC (cf. Fig. 6).

Finally, photodegradation studies ($P_{UV} = 150\,W$, $V' = 135\,m^3\,h^{-1}$) were carried out on mixtures of the saturated CHC's DCM and 1,1,1-TCA with PCE. For instance, 44 ppm DCM in 123 ppm PCE were degraded to 11 ppm with a concomitant quantitative conversion of PCE. In addition to the photooxidation products of PCE, FC was detected. DCM reacts with Cl atoms through H abstraction. The resulting dichloromethyl radical undergoes further reactions in analogy to reaction (6), after all yielding FC. The PCE degradation remained largely unaffected by the presence of the DCM component. This finding can be readily understood because (i) the rate constant of the Cl addition to PCE exceeds that of the H abstraction from DCM by Cl by 2 orders of magnitude and (ii) at the end of its reaction sequence the DCM makes restitution of the Cl atoms to the respective donor PCE. Furthermore, as compared with DCM, the reactivity of 1,1,1-TCA with Cl is lower by two further orders of magnitude. Hence, application of the same photoreaction conditions ($P_{UV} = 150\,W$, $V' = 135\,m^3\,h^{-1}$) to 1,1,1-TCA in a mixture with the strong Cl donor PCE could produce only a negligible degradation (e.g. 29 ppm 1,1,1-TCA in 121 ppm PCE was decomposed by about 2%).

4. Conclusions

Photodegradation studies of CHC's diluted in air have been carried out using a 222 nm excimer lamp. Main effort was directed towards the chlorinated ethylenes PCE and TCE in pure form and in mixtures with their natural degradation products *cis*-DCE, VC and 1,1,1-TCA, thus addressing exhaust gases from remediation of ground water and soil as a relevant problem of environmental protection. In the ranges of overall contaminant concentrations up to 250 ppm and air streams up to $450\,m^3\,h^{-1}$, the photodegradation of the highly chlorinated ethylenes proved exceedingly efficient, also mineralising the less chlorinated ones through subsequent reactions with the chain-sustaining Cl atoms.

A finite-element model of the photoreactor was devised according to the methodological pattern of fractional steps. It disclosed quite narrow reaction zones within which photodegradation efficiently occurs. In agreement with experiment, a variation of operational parameters including UV radiant power, pollutant concentration and air stream, first of all causes just a axial shift of the reaction zone. This particular finding imposes a stable degradation behaviour even under industrial conditions. The demonstrated efficiency and stability motivate an integration of the elaborated UV photodegradation route in a more complex three-step purification route, and scaling up this photolytic device to industrial applications is hopefully envisaged in future work.

Acknowledgements

This work was financially supported by Sächsisches Ministerium für Wissenschaft und Kunst und Stadtwerke Düsseldorf AG. The authors are grateful to J. Schubert (Stadtwerke Düsseldorf AG) and Prof. C. von Sonntag (Max-Planck-Institut für Strahlenchemie Mülheim) for discussions.

References

[1] L. Prager, Thesis, Leipzig University, 2000.
[2] W.R. Haag, M.D. Johnson, R. Scofield, Environ. Sci. Technol. 30 (1996) 414.
[3] E. Sanhueza, I.C. Hisatsune, J. Heicklen, Chem. Rev. 76 (1976) 801.
[4] W.G. Mallard, F. Westley, J.T. Herron, R.F. Hampson, D.H. Frizzell, NIST Chemical Kinetics Database, Version 2Q98, National Institute of Standards and Technology, Gaithersburg, 1998.
[5] H.-H. Perkampus, UV–VIS Atlas of Organic Compounds, VCH, Weinheim, 1992.

[6] A.E. Cassano, C.A. Martin, R.J. Brandi, O.M. Alfano, Ind. Eng. Chem. Res. 34 (1995) 2155.
[7] N.N. Yanyenko, The method of Fractional Steps, Springer, New York, 1971.
[8] U. Kogelschatz, in: B.M. Penetrante, S.E. Schultheis (Eds.), Non-Thermal Plasma Techniques for Pollution Controll: Electron Beam and Electrical Discharge Processing, Springer, Berlin, 1993, 939 pp.
[9] V. Catoire, P.A. Ariya, H. Niki, H.G.W. Harris, Int. J. Chem. Kinet. 29 (1997) 695.
[10] H. Scheytt, Thesis, Nürnberg — Erlangen University, 1995.